PCCP

Gas phase reactions of C_1–C_4 alcohols with the OH radical: A quantum mechanical approach

Annia Galano,* J. Raúl Alvarez-Idaboy,* Graciela Bravo-Pérez and Ma. Esther Ruiz-Santoyo

Instituto Mexicano del Petróleo, Eje Central Lázaro Cárdenas 152, 07730, México D. F., México. E-mail: jidaboy@imp.mx and agalano@imp.mx

Received 11th June 2002, Accepted 30th July 2002
First published as an Advance Article on the web 28th August 2002

CCSD(T)//BHandHLYP/6-311G(d,p) calculations have been performed to study the OH hydrogen abstraction reaction from C_1–C_4 aliphatic alcohols. A complex mechanism involving the formation of a stable pre-reactive complex is proposed and the temperature dependence of the rate coefficients is studied over the temperature range of 290–500 K, using conventional transition state theory (CTST). Excellent agreement between calculated and experimental k at 298 K has been obtained. Arrhenius expressions are proposed for 1-propanol and 1-butanol, $k_{1\text{-Prop}} = 3.06 \times 10^{-12}\exp(140/T)$ and $k_{1\text{-But}} = 2.14 \times 10^{-12}\exp(440/T)$ cm^3 molecule^{-1}·s^{-1}, respectively. The rate coefficient for the formation of the alpha radical is found significantly larger than that of the competing channels for C1–C3 alcohols. The finding that at room temperature the rate constant of 1-butanol$_\gamma$ is the largest one supports some of the previous experimental results.

Introduction

There are over 70 alcohols in the atmosphere as a result of biogenic and anthropogenic emissions.[1] Among them, the C_1–C_5 alcohols are widely used in industrial applications and are also emitted from biological processes. Methanol[2,3] and ethanol[2,4] have been used as fuels additives to reduce automobile emissions of carbon monoxide and hydrocarbons,[5] in particular ethanol has been used in Brazil as a fuel for over 20 years.[6] 1-Propanol is widely used as a solvent in the manufacturing of different electronic components. The high volatility of these compounds causes their relative abundance in the troposphere and makes it relevant to determine their degradation pathways. During daytime the major loss process for alcohols is their reaction with OH radicals.[2]

Due to their importance, the reactions of many volatile organic compounds (VOCs) with OH have been extensively studied, compilations of the kinetic data and mechanisms appear in the Atkinson *et al.*[7–9] and DeMore *et al.*[10] reviews. Several kinetic studies of alcohols + OH reactions have been performed both in purely gas phase environments[7–10] as well as in the presence of aerosols.[11] Nevertheless, there are still open questions about their reactivity and there is not at all a systematic study about the competitive reaction sites as a function of the alcohol size. Oh and Andino[11] found that the rate constants (k) of OH reaction with methanol, ethanol and 1-propanol may increase about 23–32% under atmospheric conditions due to the presence of polar aerosols, nevertheless the ks of C_4–C_6 aliphatic alcohols studied in their work remain almost unchanged. According to these authors the observed variation in the relative rate constants may be explained in terms of steric effects.

In the present work all of the possible reaction sites for hydrogen abstraction in methanol, ethanol, 1-propanol, 2-propanol and 1-butanol are studied. In Table I the kinetic parameters for these alcohols + OH radical gas phase reactions, recommended by Atkinson,[7,9] are summarized. The symbols $\Gamma_{\alpha,\beta,\gamma \text{ or } O}$ represent the branching ratios defined as $k_{\alpha,\beta,\gamma \text{ or } O}/k_{\text{total}}$, where α, β, γ or O refer to the path of OH attack.

In this study we have investigated all the possible reaction sites for hydrogen abstraction in the above-mentioned alcohols with the exception of the H_δ in the 1-butanol. This exception was made based on the consideration that the abstraction of those H atoms should be neglected compared to the other four possible channels for this molecule because they are linked to a primary carbon. The modeled reaction paths are:

$$CH_3OH + {}^\bullet OH \rightarrow C^\bullet H_2OH + H_2O \quad (1a)$$

$$\rightarrow CH_3O^\bullet + H_2O \quad (1b)$$

$$C_2H_5OH + {}^\bullet OH \rightarrow CH_3C^\bullet HOH + H_2O \quad (2a)$$

$$\rightarrow C^\bullet H_2CH_2OH + H_2O \quad (2b)$$

$$\rightarrow CH_3CH_2O^\bullet + H_2O \quad (2c)$$

$$\text{n-}C_3H_7OH + {}^\bullet OH \rightarrow CH_3CH_2C^\bullet HOH + H_2O \quad (3a)$$

$$\rightarrow CH_3C^\bullet HCH_2OH + H_2O \quad (3b)$$

$$\rightarrow C^\bullet H_2CH_2CH_2OH + H_2O \quad (3c)$$

$$\rightarrow CH_3CH_2CH_2O^\bullet + H_2O \quad (3d)$$

$$\text{i-}C_3H_7OH + {}^\bullet OH \rightarrow CH_3C^\bullet(OH)CH_3 + H_2O \quad (4a)$$

$$\rightarrow CH_3CH(OH)C^\bullet H_2 + H_2O \quad (4b)$$

$$\rightarrow CH_3CH(O^\bullet)CH_3 + H_2O \quad (4c)$$

$$\text{n-}C_4H_9OH + {}^\bullet OH \rightarrow CH_3CH_2CH_2C^\bullet HOH + H_2O \quad (5a)$$

$$\rightarrow CH_3CH_2C^\bullet HCH_2OH + H_2O \quad (5b)$$

$$\rightarrow CH_3C^\bullet HCH_2CH_2OH + H_2O \quad (5c)$$

$$\rightarrow CH_3CH_2CH_2CH_2O^\bullet + H_2O \quad (5d)$$

For each alcohol a complex system with several pathways, which move forward different transition structures to a set of various products, is present. To simplify its analysis we assumed that once a specific pathway started it proceeds to completion, independently of the other pathways, *i.e.*: there is no mixing or crossover between different pathways. On this basis, the overall rate (k) constant that measures the rate of OH disappearance, can be determined by summing up the rate

 DOI: 10.1039/b205630e

Table 1 Kinetic parameters for alcohols + OH radical gas phase reactions at 298 K, recommended by Atkinson[7,9]

	Methanol	Ethanol	1-Propanol	2-Propanol	1-Butanol
k/cm^3 molecule^{-1} s^{-1}	9.30×10^{-13}	3.20×10^{-12}	5.50×10^{-12}	5.10×10^{-12}	8.10×10^{-12}
Δk	±25%	±25%	±30%	±22%	±30%
k limits	8.00×10^{-13}	2.75×10^{-12}	4.50×10^{-12}	4.52×10^{-12}	6.63×10^{-12}
	1.08×10^{-12}	3.72×10^{-12}	6.72×10^{-12}	5.75×10^{-12}	9.89×10^{-12}
E^{Arr}/kcal mol^{-1}	0.72 ± 0.40	0.14 ± 0.40	—	0.38 ± 0.40	—
A/cm^3 molecule^{-1} s^{-1}	3.10×10^{-12}	4.10×10^{-12}	—	2.70×10^{-12}	—
Γ_α[b]	0.85 ± 0.10	$0.90^{+0.10}_{-0.05}$	$0.48 - 0.73$	—	—
Γ_β	—	$0.05^{+0.10}_{-0.05}$	—	0.12[a]	—
Γ_γ	—	—	—	—	—
Γ_O	0.15 ± 0.10	$0.05^{+0.10}_{-0.05}$	—	—	—

[a] Ref. 65. [b] $\Gamma_{\alpha,\beta,\gamma \text{ or } O}$ = Branching ratio = $k_{\alpha,\beta,\gamma \text{ or } O}/k_{total}$

coefficients calculated for all of each different pathways.[12] In addition in this paper the temperature dependence of k was also studied and calculated Arrhenius parameters are presented.

Computational methods

Electronic structure calculations have been performed with the Gaussian 98[13] program. Full geometry optimizations were made for all the stationary points using the BHandHLYP hybrid HF-density functional[14] and the 6-311G(d,p) basis set. This functional was chosen on the base of its proven effectiveness,[15–24] and the energies were improved by single point calculations at CCSD(T)/6-311G(d,p) level. Restricted calculations were used for closed shell systems and unrestricted ones for open shell systems.

Frequency calculations were carried out for all the stationary points at the corresponding level of theory. local minima and transition states were identified by the number of imaginary frequencies (NIMAG = 0 or 1, respectively). In addition, the vibrational modes with imaginary frequency were inspected using the GaussView program, and it was confirmed that they do connect the corresponding reactants and products. Zero point energies (ZPE) and thermal corrections to the energy (TCE) were included in the determination of energy barriers.

The conventional transition state theory (CTST) methodology,[25,26] implemented in the Rate 1.1 program,[27] was used to calculate the rate coefficients since it has the advantage of being non-expensive for a high level of *ab initio* calculations. It is known that CTST does not include the recrossing effects, which are important in the high-temperature region for reactions with low barriers; however, the alcohol + OH reaction has relative high barriers and are not in the high-temperature region, this is discussed in a latter section. Consequently the CTST is adequate to describe this reaction.

The tunneling correction defined as the Boltzmannn average of the ratio of the quantum and the classical probabilities were calculated using the Eckart method.[28] This method approximates the potential by a one-dimensional function that is fitted to reproduce the zero-point energy corrected barrier, the enthalpy of reaction at 0 K, and the curvature of the potential curve at the transition state and it can be considered as a special case of the zero-curvature tunneling (ZCT) calculation. This method tends to overestimate the tunneling contribution, especially at very low temperature, because the fitted Eckart function is often too narrow. However, sometimes it compensates for the corner-cutting effect not included in the Eckart approach.[29–31] Such compensation can lead to Eckart transmission coefficients similar[30] or even lower[31] at 300 K than those obtained by the small-curvature tunneling (SCT) method.[32]

Molecular structures

CH_3OH + OH System

A pre-reactive complex was found (**RC-M** in Fig. 1) with the methanol structure almost identical to the free molecule. The only difference was a slight elongation (0.01 Å) of the C_α–O_I bond. The **RC-M** formation is caused by the interaction between the H atom in the OH radical and the O atom in the methanol, they are 1.84 Å apart, which represents a hydrogen bond interaction and is responsible for the stabilization.

Two transition states were found: HO···H···CH_2OH (**TS-M_α**) and CH_3O···H···OH (**TS-M_O**), depending on the H atom in methanol to be abstracted (Fig. 1). Two major changes occur due to the **TS-M_α** formation, the H_α-C_α bond elongation by 0.11 Å and the C_α-O_I bond shortening by 0.02 Å. The H-attack on the methyl side was found to be on the antihydrogen of CH_3 (regarding to OH orientation) and almost collinear with the $C_\alpha H_\alpha O_{II}$ angle, equal to 167.8°. This result is consistent with previous optimizations performed for this system at MP2/6-311G(d,p) level.[33] A very weak interaction was found between the H atom in the OH radical and O atom in the methanol, with the distance between them equal to 3.27 Å. A hydrogen bond molecular complex H_2O···$HOCH_2$ (**PC-M_α** in Fig. 1) was found in the exit channel, with the O_{II}···H_{OI} distance equal to 1.82 Å and the $O_{II}H_{OI}O_I$ angle equal to 176.7°.

The most relevant structural changes related to the **TS-M_O** formation, were the H_{OI}-O_I bond elongation by 0.14 Å and

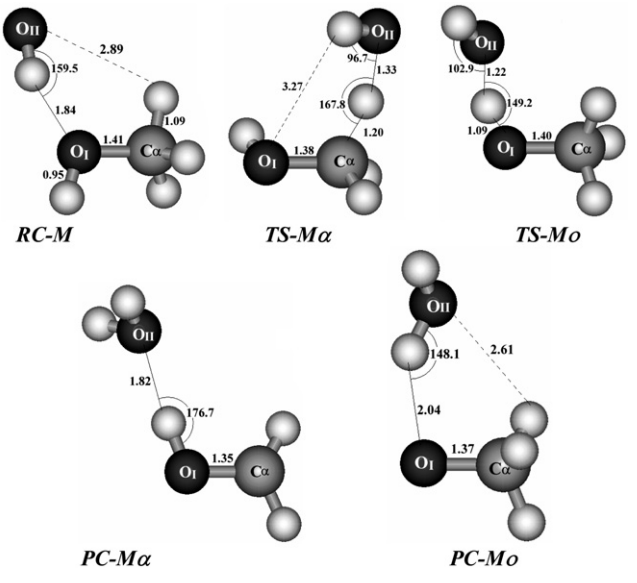

Fig. 1 Structures of some stationary points for the OH hydrogen abstraction reaction from CH_3OH (**M**).

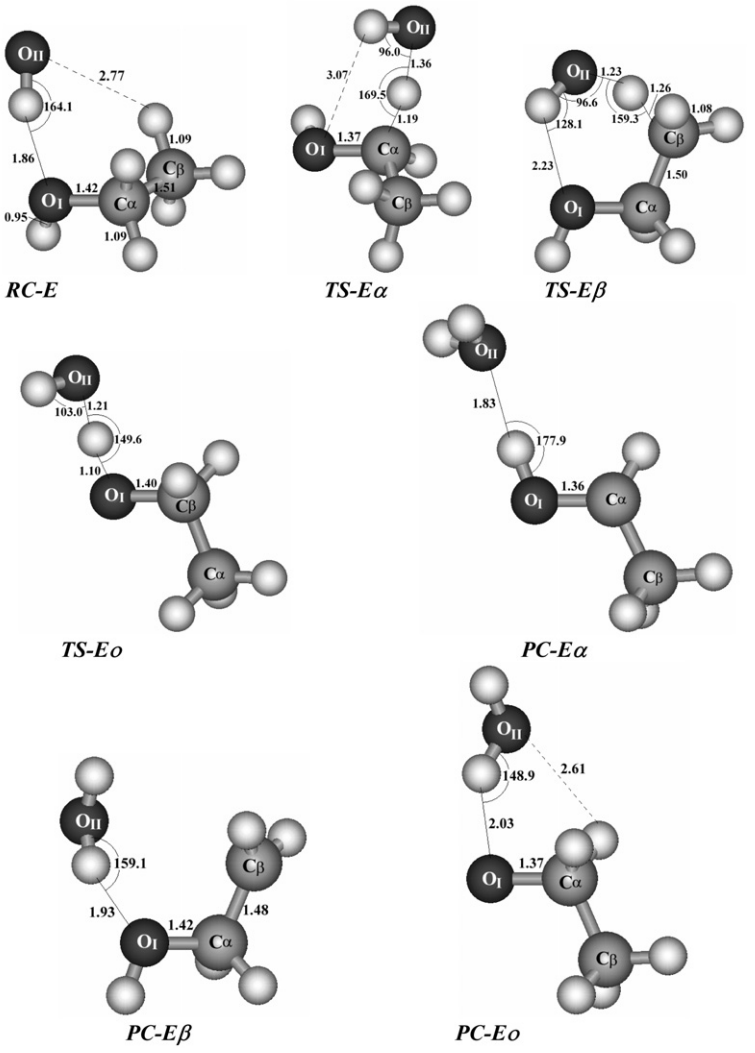

Fig. 2 Structures of some stationary points for the OH hydrogen abstraction reaction from C_2H_5OH (**E**).

the C_α-O_1 bond shortening by 0.01 Å. The attack of the OH radical on the hydroxyl side was found to be bent, with the $O_{II}H_{OI}O_I$ angle equal to 149.2°. For this channel a weaker hydrogen bond molecular complex $HOH\cdots OCH_3$ (**PC-M$_O$** in Fig. 1) was also found in the exit channel, with the $H_{OII}\cdots O_I$ distance equal to 2.04 Å and the $O_{II}H_{OII}O_I$ angle equal to 148.1°.

C_2H_5OH + OH System

A pre-reactive complex caused by the interaction between the H atom in the OH radical and the O atom in the ethanol was found (**RC-E** in Fig. 2). In this complex the ethanol remains practically unchanged compared to the free molecule, the only difference was a slight elongation (0.01 Å) of the C_α–O_I bond. The atoms involved in the **RC-E** formation are 1.86 Å apart, which is a hydrogen bond interaction and is responsible for the stabilization.

In this system three transition states were found: $CH_3CH(H\cdots OH)OH$ (**TS-E$_\alpha$**), $HO\cdots H\cdots CH_2CH_2OH$ (**TS-E$_\beta$**) and $C_2H_5O\cdots H\cdots OH$ (**TS-E$_O$**), whose formation depends on the H atom to be abstracted from ethanol (Fig. 2). Two major changes occur in the **TS-E$_\alpha$** formation, the H_α–C_α bond elongation by 0.10 Å and the C_α–O_I bond shortening by 0.04 Å. A slight shortening of the C_α–C_β bond by 0.01 Å is present. The H-attack on the alpha hydrogen was found nearly collinear, with the $C_\alpha H_\alpha O_{II}$ angle equal to 169.5°. A very weak interaction was found between the H atom in the OH radical and O atom in the ethanol at a distance of 3.07 Å. In the exit channel A hydrogen bond molecular complex $H_2O\cdots HOCHCH_3$ (**PC-E$_\alpha$** in Fig. 2) was found, the $O_{II}\cdots H_{OI}$ distance is equal to 1.83 Å and the $O_{II}H_{OI}O_I$ angle equal to 177.9°.

The major changes due to the **TS-E$_\beta$** formation were the H_β–C_β bond elongation by 0.17 Å and a slight shortening of the C_α-C_β bond by 0.01 Å. The H-attack on the beta hydrogen was found almost collinear, with the $C_\beta H_\beta O_{II}$ angle equal to 169.5°. A weak attractive interaction was found between the H atom in the OH radical and O atom in the ethanol, with the distance between them equal to 2.23 Å. A hydrogen bond molecular complex $HOH\cdots OHCH_2CH_2$ (**PC-E$_\beta$** in Fig. 2) was found in the exit channel, with the $H_{OII}\cdots O_I$ distance equal to 1.93 Å and the $O_{II}H_{OII}O_I$ angle equal to 159.1°.

The most relevant structural changes, due to the **TS-E$_O$** formation, were the H_{OI}-O_I bond elongation by 0.15 Å and the C_α-O_1 bond shortening by 0.01 Å. The attack of the OH radical on the hydroxyl side was found to be non-collinear, with the $O_{II}H_{OI}O_I$ angle equal to 149.6°. For this channel a weaker hydrogen bond molecular complex $HOH\cdots OCH_2CH_3$ (**PC-E$_O$** in Fig. 2) was also found in the exit channel, with the $H_{OII}\cdots O_I$ distance equal to 2.03 Å and the $O_{II}H_{OII}O_I$ angle equal to 148.9°.

C_3H_7OH + OH System

A pre-reactive complex was found (**RC-nP** in Fig. 3) by the interaction between the H atom in the OH radical and the O

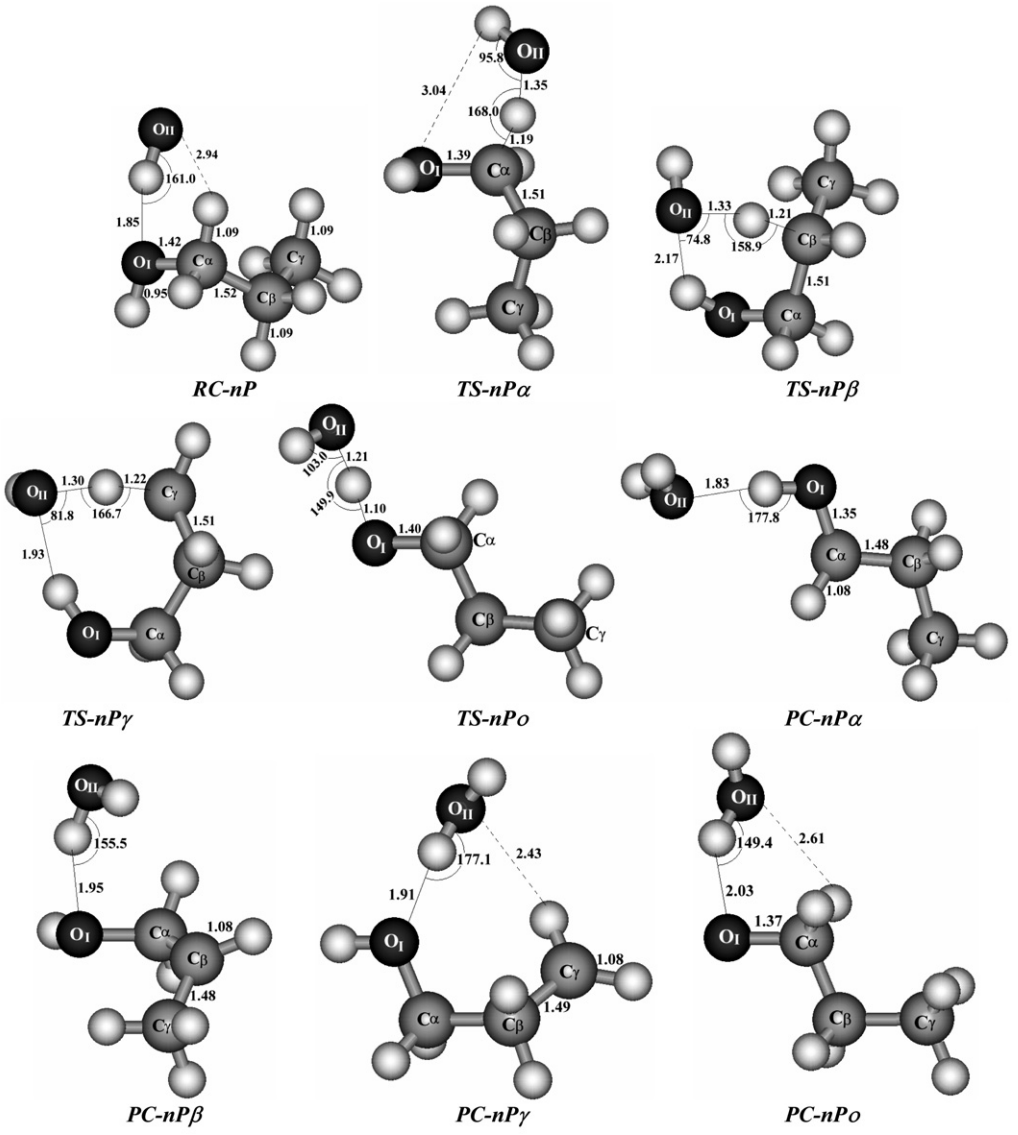

Fig. 3 Structures of some stationary points for the OH hydrogen abstraction reaction from n-C_3H_7OH (**nP**).

atom in the 1-propanol. The 1-propanol structure remains nearly unchanged compared to the free molecule; the only difference was a slight elongation (0.01 Å) of the C_α–O_I bond. The atoms involved in the **RC-nP** formation are 1.85 Å apart, which is a hydrogen bond interaction and is responsible for the stabilization.

For this system four transition states were found: $CH_3CH_2CH(H\cdots OH)OH$ (**TS-nP$_\alpha$**), $CH_3CH(H\cdots OH)CH_2$-OH (**TS-nP$_\beta$**), $HO\cdots H\cdots CH_2CH_2CH_2OH$ (**TS-nP$_\gamma$**) and $C_3H_7O\cdots H\cdots OH$ (**TS-nP$_O$**), depending on the H atom in 1-propanol to be abstracted (Fig. 3). Two major changes occur due to the **TS-nP$_\alpha$** formation: the H_α-C_α bond elongation by 0.10 Å and the C_α-O_I bond shortening by 0.02 Å. The H-attack on the alpha hydrogen was found practically collinear, with the $C_\alpha H_\alpha O_{II}$ angle equal to 168.0°. A very weak interaction was found between the H atom in the OH radical and O atom in the 1-propanol, with the distance between them equal to 3.04 Å. A hydrogen bond molecular complex $H_2O\cdots HO$-$CHCH_2CH_3$ (**PC-nP$_\alpha$** in Fig. 3) was found in the exit channel, with the $O_{II}\cdots H_{OI}$ distance equal to 1.83 Å and the $O_{II}H_{OI}O_I$ angle equal to 177.8°.

The major change due to the **TS-nP$_\beta$** formation was the H_β-C_β bond elongation by 0.12 Å. The H-attack on the beta hydrogen was found to be bent, with the $C_\beta H_\beta O_{II}$ angle equal to 158.9°. A weak attractive interaction was found between the H atom in the OH group in 1-propanol and the O atom in the OH radical, with the distance between them equal to 2.17 Å. A hydrogen bond molecular complex $HOH\cdots OHCH_2CHCH_3$ (**PC-nP$_\beta$** in Fig. 3) was found in the exit channel, with the $H_{OII}\cdots O_I$ distance equal to 1.95 Å and the $O_{II}H_{OII}O_I$ angle equal to 155.5°.

The most significant change due to the **TS-nP$_\gamma$** formation was the H_γ-C_γ bond elongation by 0.13 Å. The H-attack on the gamma hydrogen was found nearly collinear, with the $C_\gamma H_\gamma O_{II}$ angle equal to 166.7°. An attractive interaction was found between the H atom in the OH group in 1-propanol and the O atom in the OH radical, with the distance between them equal to 1.93 Å. A hydrogen bond molecular complex $HOH\cdots OHCH_2CH_2CH_2$ (**PC-nP$_\gamma$** in Fig. 3) was found in the exit channel, with the $H_{OII}\cdots O_I$ distance equal to 1.91 Å and the $O_{II}H_{OII}O_I$ angle equal to 177.1°. A weak interaction was also found in **PC-nP$_\gamma$** between an H atom in the gamma carbon and the O atom in the water molecule, with the $H_\gamma\cdots O_{II}$ distance equal to 2.43 Å.

The most relevant structural changes due to the **TS-nP$_O$** formation were the H_{OI}-O_I bond elongation by 0.15 Å and the C_α-O_1 bond shortening by 0.01 Å. The attack of the OH radical on the hydroxyl side was found to be non-collinear, with the $O_{II}H_{OI}O_I$ angle equal to 149.9°. For this channel a weaker hydrogen bond molecular complex $HOH\cdots OCH_2CH_2CH_3$

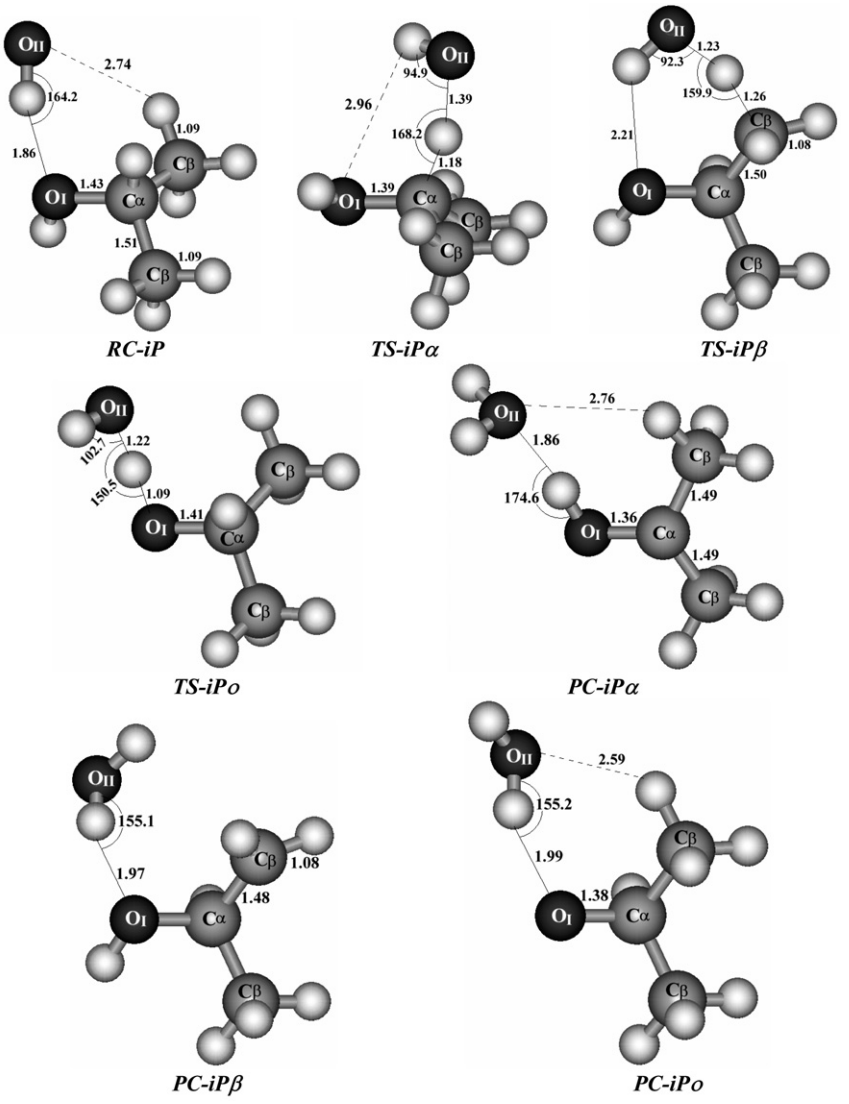

Fig. 4 Structures of some stationary points for the OH hydrogen abstraction reaction from i-C_3H_7OH (**iP**).

(**PC-nP$_O$** in Fig. 3) was also found in the exit channel, with the $H_{OII}\cdots O_I$ distance equal to 2.03 Å and the $O_{II}H_{OII}O_I$ angle equal to 149.4°.

$CH_3CH(OH)CH_3$ + OH system

The pre-reactive complex caused by the interaction between the H atom in the OH radical and the O atom in the 2-propanol (**RC-iP**) is shown in Fig. 4. The 2-propanol structure is almost unchanged compared to the free molecule; the only difference was a slight elongation (0.02 Å) of the C_α-O_I bond. The atoms involved in the **RC-iP** formation are 1.86 Å apart, which is a hydrogen bond interaction and is responsible for the stabilization.

In this case three transition states were found: $(CH_3)_2C(H\cdots OH)OH$ (**TS-iP$_\alpha$**), $HO\cdots H\cdots CH_2CH(OH)CH_3$ (**TS-iP$_\beta$**) and $(CH_3)_2CHO\cdots H\cdots OH$ (**TS-iP$_O$**), depending on the H atom in 2-propanol to be abstracted (Fig. 4). Two major changes occur due to the **TS-iP$_\alpha$** formation, the H_α–C_α bond elongation by 0.09 Å and the C_α-O_I bond shortening by 0.02 Å. The H-attack on the alpha hydrogen was found nearly collinear, with the $C_\alpha H_\alpha O_{II}$ angle equal to 168.2°. A very weak interaction was found between the H atom in the OH radical and O atom in the 2-propanol, with the distance between them equal to 2.96 Å. In addition a $H_{OII}O_{II}C_\alpha O_I$ dihedral angle equal to −37.5° was found, which is in excellent agreement with a previous conformer optimization performed at MP2/6-31G*.[34] A hydrogen bond molecular complex $H_2O\cdots HOC(CH_3)_2$ (**PC-iP$_\alpha$** in Fig. 4) was found in the exit channel, with the $O_{II}\cdots H_{OI}$ distance equal to 1.86 Å and the $O_{II}H_{OI}O_I$ angle equal to 174.6°.

The major changes due to the **TS-iP$_\beta$** formation were the H_β-C_β bond elongation by 0.17 Å and a slight shortening of the C_α-C_β bond by 0.01 Å. The H-attack on the beta hydrogen was found to be non-collinear, with the $C_\beta H_\beta O_{II}$ angle equal to 159.9°. In the 2-propanol a weak attractive interaction between the H atom in the OH radical and O atom was found, the distance between them is 2.21 Å. In addition the $H_{OII}O_{II}C_\beta C_\alpha$ dihedral angle was found equal to 38.2°, which is also in very good agreement with the conformational study developed in ref. 34. A hydrogen bond molecular complex $HOH\cdots OHCH(CH_2)CH_3$ (**PC-iP$_\beta$** in Fig. 4) was found in the exit channel, with the $H_{OII}\cdots O_I$ distance equal to 1.97 Å and the $O_{II}H_{OII}O_I$ angle equal to 155.1°.

The most relevant structural change, due to the **TS-iP$_O$** formation, was the H_{OI}–O_I bond elongation by 0.14 Å. The attack of the OH radical on the hydroxyl side was found to be bent, with the $O_{II}H_{OI}O_I$ angle equal to 150.5°. In addition the $H_{OII}O_{II}O_IC_\alpha$ dihedral angle was found equal to −106.5°, which also agrees well with the results of ref. 34. for this

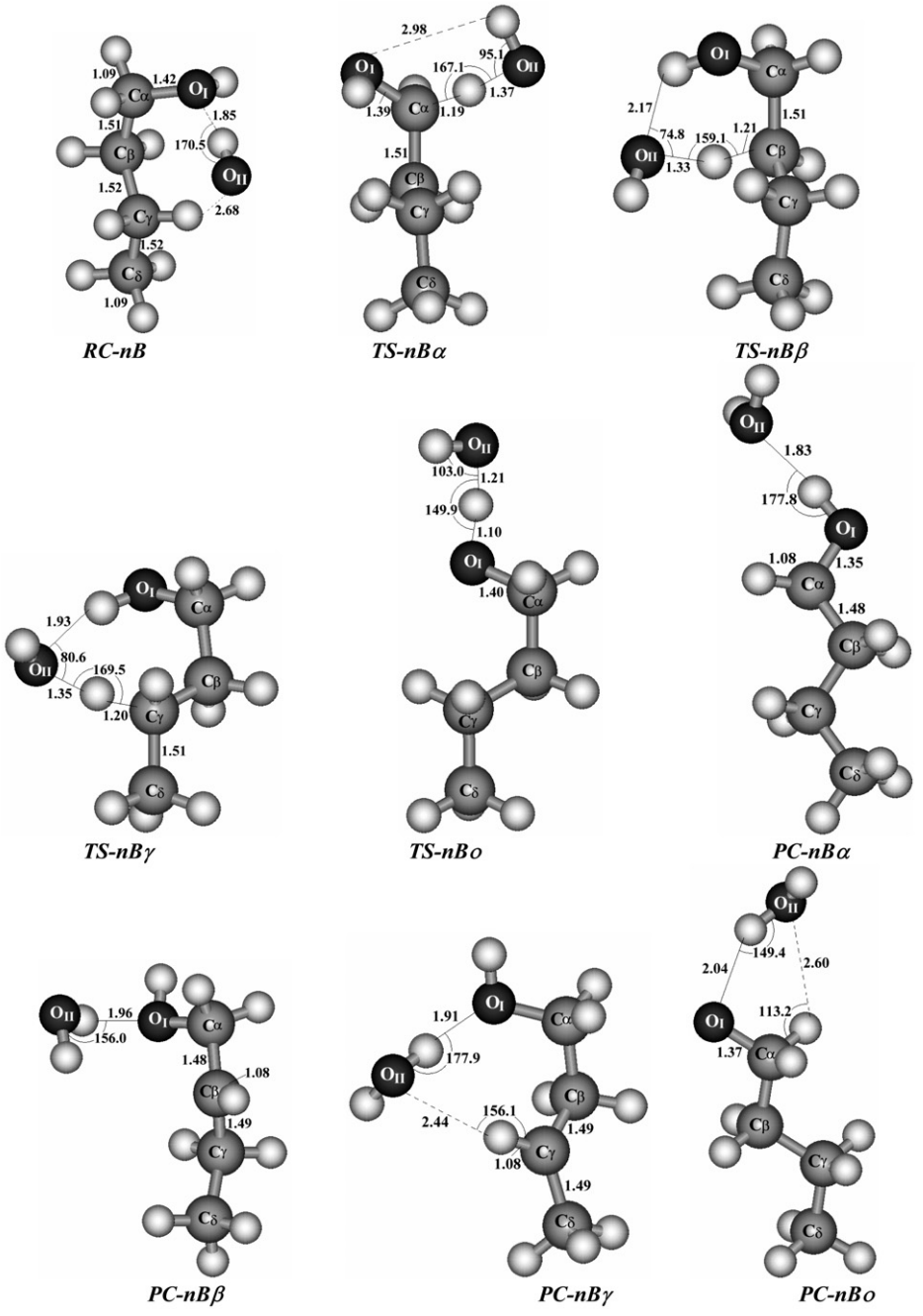

Fig. 5 Structures of some stationary points for the OH hydrogen abstraction reaction from n-C_4H_9OH (**nB**).

channel a hydrogen bond molecular complex $HOH\cdots OCH(CH_3)_2$ (**PC-iP$_O$** in Fig. 4) was also found in the exit channel, with the $H_{OII}\cdots O_I$ distance equal to 1.99 Å and the $O_{II}H_{OII}O_I$ angle equal to 155.2°.

C_4H_9OH + OH system

A pre-reactive complex was found (**RC-nB** in Fig. 5) caused by the interaction between the H atom in the OH radical and the O atom in the 1-butanol. The 1-butanol structure is nearly unchanged compared to the free molecule; the only difference was a slight elongation (0.01 Å) of the C_α-O_I bond. The atoms involved in the **RC-nB** formation are 1.85 Å apart, which is a hydrogen bond interaction and is responsible for the stabilization. An additional and weaker interaction was found between the O atom in the OH radical and one of the H linked to C_γ. For this system four transition states were found: $CH_3CH_2CH_2$-$CH(H\cdots OH)OH$ (**TS-nB$_\alpha$**), $CH_3CH_2CH(H\cdots OH)CH_2OH$ (**TS-nB$_\beta$**), $CH_3CH(H\cdots OH)CH_2CH_2OH$ (**TS-nB$_\gamma$**) and $C_4H_9O\cdots H\cdots OH$ (**TS-nB$_O$**), depending on the H atom in 1-butanol to be abstracted (Fig. 5). Two major changes occur due to the **TS-nB$_\alpha$** formation: the H_α-C_α bond elongation by 0.10 Å and the C_α-O_I bond shortening by 0.02 Å. The H-attack on the alpha hydrogen was found nearly collinear, with the $C_\alpha H_\alpha O_{II}$ angle equal to 167.1°. A very weak interaction was found between the H atom in the OH radical and O atom in the 1-butanol, with the distance between them equal to 2.98 Å. A hydrogen bond molecular complex $H_2O\cdots HOCHCH_2$-CH_2CH_3 (**PC-nB$_\alpha$** in Fig. 5) was found in the exit channel, with the $O_{II}\cdots H_{OI}$ distance equal to 1.83 Å and the $O_{II}H_{OI}O_I$ angle equal to 177.8°.

The major change due to the **TS-nB$_\beta$** formation was the H_β-C_β bond elongation by 0.12 Å. The H-attack on the beta hydrogen was found to be non-collinear, with the $C_\beta H_\beta O_{II}$ angle equal to 159.1°. A weak attractive interaction was found between the H atom in the OH group in 1-butanol and the

O atom in the OH radical, with the distance between them equal to 2.17 Å. A hydrogen bond molecular complex $HOH\cdots OHCH_2CHCH_2CH_3$ (**PC-nB$_\beta$** in Fig. 5) was found in the exit channel, with the $H_{OII}\cdots O_I$ distance equal to 1.96 Å and the $O_{II}H_{OII}O_I$ angle equal to 156.0°.

The most significant change due to the **TS-nB$_\gamma$** formation was the H_γ-C_γ bond elongation by 0.11 Å. The H-attack on the gamma hydrogen was found nearly collinear, with the $C_\gamma H_\gamma O_{II}$ angle equal to 169.5°. An attractive interaction was found between the H atom in the OH group in 1-butanol and the O atom in the OH radical, with the distance between them equal to 1.93 Å. A hydrogen bond molecular complex $HOH\cdots OHCH_2CH_2CHCH_3$ (**PC-nB$_\gamma$** in Fig. 5) was found in the exit channel, with the $H_{OII}\cdots O_I$ distance equal to 1.91 Å and the $O_{II}H_{OII}O_I$ angle equal to 177.9°. A weak interaction was also found in **PC-nB$_\gamma$** between an H atom in the gamma carbon and the O atom in the water molecule, with the $H_\gamma\cdots O_{II}$ distance equal to 2.44 Å.

The most relevant structural changes due to the **TS-nB$_O$** formation were the H_{OI}-O_I bond elongation by 0.15 Å and the C_α-O_1 bond shortening by 0.01 Å. The attack of the OH radical on the hydroxyl side was found to be bent, with the $O_{II}H_{OI}O_I$ angle equal to 149.9°. For this channel a weaker hydrogen bond molecular complex $HOH\cdots OCH_2CH_2CH_2CH_3$ (**PC-nB$_O$** in Fig. 5) was also found in the exit channel, with the $H_{OII}\cdots O_I$ distance equal to 2.04 Å and the $O_{II}H_{OII}O_I$ angle equal to 149.4°.

Energies and mechanisms

The absolute energies of the most relevant optimized stationary points, as well as the relative energies with respect to reactants including ZPE corrections, and the *L* parameters are reported in Table 2. The *L* parameter indicates whether a transition state structure is reactant-like ($L<1$) or product-like ($L>1$) and also quantifies the corresponding trend. Consequently there must be a direct relation between the *L* value and the heat of reaction of a specific pathway, according to the Hammond postulate. *L* parameters were

Table 2 Absolute energies (Hartrees), zero point energy corrections (ZPE) (Hartrees), relative energies with respect to reactants (kcal mol^{-1}) including ZPE corrections; and the *L* parameter

Molecular system	Absolute energies		ZPE	Relative energies	*L*
	BH&HLYP	CCSD(T)		CCSD(T)	
$CH_3OH + OH$	−191.410325	−191.057179	0.061913		
RC-M	−191.424219	−191.069495	0.065099	−5.73	
TS-M$_\alpha$	−191.404266	−191.051869	0.059887	2.06	0.31
PC-M$_\alpha$	−191.402175	−191.049865	0.059561	−24.95	
TS-M$_O$	−191.449089	−191.099016	0.063995	3.11	0.55
PC-M$_O$	−191.438768	−191.083933	0.063799	−15.60	
$C_2H_5OH + OH$	−230.713875	−230.274912	0.091491		
RC-E	−230.728401	−230.288904	0.095051	−6.55	
TS-E$_\alpha$	−230.710058	−230.272079	0.089346	0.43	0.25
PC-E$_\alpha$	−230.705155	−230.268961	0.089655	−25.79	
TS-E$_\beta$	−230.705077	−230.267761	0.089072	2.58	0.61
PC-E$_\beta$	−230.754608	−230.317826	0.093314	−16.26	
TS-E$_O$	−230.737640	−230.301733	0.092394	2.97	0.57
PC-E$_O$	−230.741853	−230.301508	0.093121	−15.67	
$n\text{-}C_3H_7OH + OH$	−270.011832	−269.488827	0.121161		
RC-nP	−270.025850	−269.501980	0.124286	−6.29	
TS-nP$_\alpha$	−270.007841	−269.486194	0.118889	0.23	0.27
PC-nP$_\alpha$	−270.007818	−269.487331	0.119481	−24.92	
TS-nP$_\beta$	−270.006446	−269.485354	0.119667	0.91	0.33
PC-nP$_\beta$	−270.002439	−269.480495	0.118468	−19.12	
TS-nP$_\gamma$	−270.051813	−269.530228	0.122850	1.73	0.39
PC-nP$_\gamma$	−270.042131	−269.520493	0.122364	−17.75	
TS-nP$_O$	−270.039689	−269.518711	0.122760	3.54	0.57
PC-nP$_O$	−270.039284	−269.514226	0.122672	−14.99	
$i\text{-}C_3H_7OH + OH$	−270.016989	−269.494216	0.120284		
RC-iP	−270.031406	−269.508017	0.123730	−6.50	
TS-iP$_\alpha$	−270.014910	−269.493613	0.118310	−0.86	0.21
PC-iP$_\alpha$	−270.008363	−269.488633	0.118394	−26.08	
TS-iP$_\beta$	−270.008330	−269.487708	0.117798	2.32	0.62
PC-iP$_\beta$	−270.059465	−269.537824	0.122333	−16.72	
TS-iP$_O$	−270.041498	−269.522146	0.121576	2.52	0.54
PC-iP$_O$	−270.044987	−269.521262	0.122765	−15.41	
$n\text{-}C_4H_9OH + OH$	−309.323048	−308.714229	0.153802		
RC-nB	−309.305370	−308.699507	0.148566	−6.00	
TS-nB$_\alpha$	−309.304419	−308.699573	0.148523	−0.05	0.25
PC-nB$_\alpha$	−309.305951	−308.700178	0.148332	−24.93	
TS-nB$_\beta$	−309.299826	−308.693610	0.147862	−0.11	0.47
PC-nB$_\beta$	−309.348994	−308.742750	0.152152	−18.98	
TS-nB$_\gamma$	−309.339088	−308.732899	0.151781	−0.61	0.28
PC-nB$_\gamma$	−309.341541	−308.734769	0.151762	−20.17	
TS-nB$_O$	−309.336470	−308.726782	0.152034	3.21	0.58
PC-nB$_O$	−309.323048	−308.714229	0.153802	−14.98	

calculated for each modeled channel following ref. 35 and 36 as:

$$L_\alpha = \frac{\delta r(C_\alpha H_\alpha)}{\delta r(H_\alpha O_{II})} \quad (1)$$

$$L_\beta = \frac{\delta r(C_\beta H_\beta)}{\delta r(H_\beta O_{II})} \quad (2)$$

$$L_\gamma = \frac{\delta r(C_\gamma H_\gamma)}{\delta r(H_\gamma O_{II})} \quad (3)$$

and

$$L_O = \frac{\delta r(O_I H_{O_i})}{\delta r(H_{O_i} O_{II})} \quad (4)$$

In these equations, $\delta r(C_\alpha H_\alpha)$, $\delta r(C_\beta H_\beta)$, $\delta r(C_\gamma H_\gamma)$, and $\delta r(O_I H_{O_i})$ represent the variation in the breaking bond distance between transition states and reactants, along the different channels, while $\delta r(H_\alpha O_{II})$, $\delta r(H_\beta O_{II})$, $\delta r(H_\gamma O_{II})$, and $\delta r(H_{O_i} O_{II})$ represent the variation in the forming bond distance between transition states and products.

As expected, all the modeled channels were found exothermic (Table 2), and all the L parameters <1. Besides, for all the studied alcohols the alpha channel is the most exothermic one and also corresponds to the earliest transition state of each alcohol.

According to the energy barriers (E^*) reported in the same table, the alpha channel is the most likely to occur for the alcohols from C1 to C3, but for 1-butanol the gamma channel barrier is about 0.56 kcal mol^{-1} lower than the alpha one, and even the beta E^* is slightly lower than the $E^*(\alpha)$, suggesting that gamma abstraction is the dominant path for this alcohol. This lowest abstraction energy barrier for the gamma channel is in apparent contradiction with the finding that L_α is lower than L_γ (Table 2), yet the explanation is related to the transition structure, as will be discussed latter. In addition all the heights of the apparent reaction barrier, *i.e.* with respect to reactants, are very low and some of them are slightly negative.

As shown in Fig. 6 the mechanism of the alcohol + OH reaction seems to be a two step mechanism involving a reactant complex (RC) formation (**RC-M**, **RC-E**, **RC-nP**, **RC-iP** and **RC-nB**). The rather large OH radical electric dipole moment (1.668 D) amply justifies its capability of forming strong hydrogen bonds. The high stabilization energies for all the abstraction paths (about 6 kcal mol^{-1}, Table 2) prove that and show unambiguously, that the mechanism of each reaction channel is complex with a first step leading to the RC formation and a second step yielding the corresponding radical and water. The proposed mechanism is:

$$\text{Step A: } ROH + OH^\bullet \underset{k_{-1}}{\overset{k_1}{\rightleftharpoons}} [ROH\cdots OH^\bullet] \quad (I)$$

$$\text{Step B: } [ROH\cdots OH^\bullet] \xrightarrow{k_2} [RO^\bullet] + H_2O \quad (II)$$

The second step energy barriers are all positive and higher than 5.5 kcal mol^{-1} for all the studied cases (Table 3), suggesting that the tunneling effect can be relevant in the C_1 to C_4 alcohol + OH reactions.

Some experimental works have been carried out to study reactant complexes involving the OH radical.[37,38] In addition, the role of hydrogen-bonded intermediates in the bimolecular reactions of the hydroxyl radical has been recently reviewed[39] and it has been established that the presence of an attractive well in the entrance channel of a potential energy surface can influence the dynamics, and hence the course, of the reaction. Its existence can manifest itself in terms of negative temperature dependence, which is to be expected when there is an attractive encounter between reactants. Another general feature of reactions involving this kind of intermediates is that the potential barrier separating the complex from the products should not be too far above the energies of the reactants nor so wide as to prevent tunneling through it. The presence of reactant complexes in OH reactions has also been theoretically studied[24,40–44] and the kinetic parameters obtained assuming that mechanism show excellent agreement with the experimental values.

Rate coefficients

The rate constant of all the studied reaction channels can be analyzed in terms of CTST. According to the reaction mechanism proposed above, if k_1 and k_{-1} are the forward and reverse rate constants for the first step and k_2 corresponds to the second step, a steady-state analysis leads to a rate coefficient for each overall reaction channel which can be written as:

$$k = \frac{k_1 k_2}{k_{-1} + k_2} \quad (5)$$

Even though the energy barrier for k_{-1} is about the same size as that for k_2, the entropy change is much larger in the reverse reaction than in the formation of the products. Thus, a k_{-1} should be expected considerably larger than k_2. Based on this assumption, first considered by Singleton and Cvetanovic,[45] k can be rewritten as:

$$k = \frac{k_1 k_2}{k_{-1}} = \left(\frac{A_1 A_2}{A_{-1}}\right) \exp\left[-\left(E_1^* + E_2^* - E_{-1}^*\right)/RT\right] \quad (6)$$

where E_1^* and E_{-1}^* are the step 1 energy barriers, corresponding to the forward and reverse directions, respectively.

Since E_1^* is zero, the net (or apparent) energy barrier for the overall reaction channel is:

$$E^* = E_2^* - E_{-1}^* = (E_{TS} - E_{RC}) - (E_R - E_{RC}) = E_{TS} - E_R \quad (7)$$

where E_{TS}, E_{RC} and E_R are the total energies of the transition state, the reactant complex and the reactants, respectively.

Applying basic statistical thermodynamic principles the equilibrium constant (k_1/k_{-1}) of the fast pre-equilibrium between the reactants and the reactant complex may be obtained as:

$$K_{eq} = \frac{Q_{RC}}{Q_R} \exp[(E_R - E_{RC})/RT] \quad (8)$$

where Q_{RC} and Q_R represent the partition functions corresponding to the reactant complex and the isolated reactants, respectively.

Under high-pressure conditions, an equilibrium distribution of reactants is maintained in a unimolecular process and the CTST formula can be applied[46] to calculate k_2:

$$k_2 = \kappa_2 \frac{k_B T}{h} \frac{Q_{TS}}{Q_{RC}} \exp[(E_{RC} - E_{TS})/RT] \quad (9)$$

where κ_2 is the tunneling factor, k_B and h are the Boltzmann and Planck constants, respectively, and Q_{TS} represents the transition state partition function. The energy differences include the ZPE corrections. The effective rate coefficient of each channel is then obtained as:

$$k = \sigma K_{eq} k_2 \quad (10)$$

where σ is the symmetry factor, which is related to the reaction path degeneracy and its value depends on the H atom to be abstracted. The symmetry factor is obtained by imaging all identical atoms to be labeled and by counting the number of different but equivalent arrangements that can be made by rotating (but not reflecting) the molecule.[47]

Finally, the overall rate constant (k) for each alcohol can be determined by summing the rate coefficients calculated for the different modeled pathways.[12] The k values were calculated

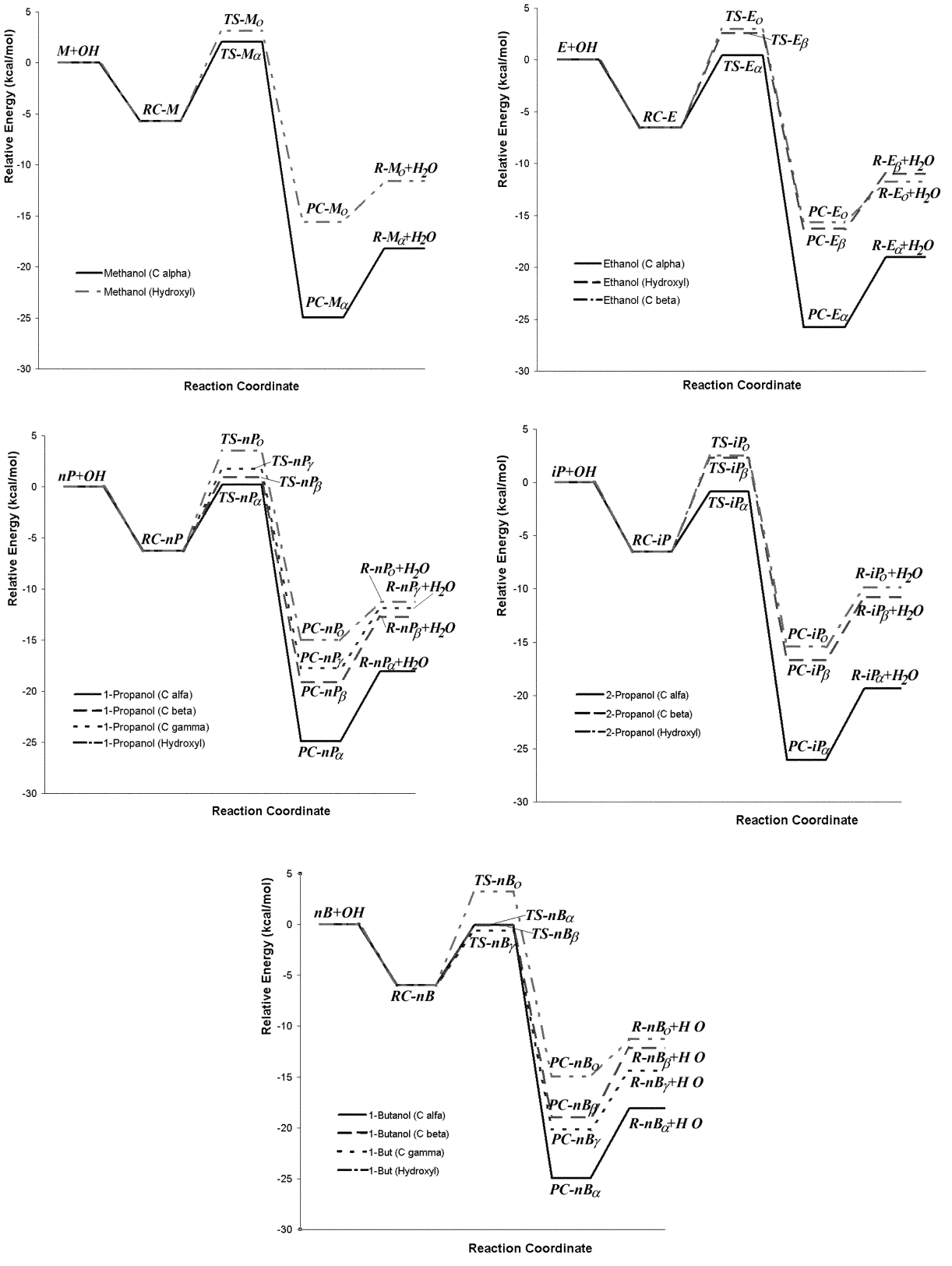

Fig. 6 Energetic profiles for the OH hydrogen abstraction reaction from C_1 to C_4 aliphatic alcohols.

over the temperature range 290–500 K and the obtained values are reported in Table 4. The excellent agreement between the calculated and experimental values at 298 K is shown in Fig 7.

In order to compare with the experimental data available, a study of the overall rate coefficient dependence on temperature was performed and the Arrhenius parameters were determined (Table 5) for all the studied alcohols. A correlation between the calculated (E^{Arr}_{Calc}) and the recommended (E^{Arr}_{Exp}) Arrhenius activation energies were performed and the best fit equation was found to be $E^{Arr}_{Calc} = 1.0174\ E^{Arr}_{Exp} - 0.2485$, with a correlation coefficient (R^2) equal to 0.98. The slope value, almost equal to 1, supports the quality of our results and allows to predict expectable values of this magnitude, for those alcohols which has no reported E^{Arr}, by correcting with the correlation equation the values calculated with the methodology described here.

Table 3 Relative energies with respect to reactant complexes (kcal mol^{-1}), including ZPE corrections

Molecular system	Relative energies CCSD(T)
TS-M$_\alpha$	7.79
PC-M$_\alpha$	−19.22
TS-M$_O$	8.84
PC-M$_O$	−9.88
TS-E$_\alpha$	6.98
PC-E$_\alpha$	−19.24
TS-E$_\beta$	9.13
PC-E$_\beta$	−9.72
TS-E$_O$	9.52
PC-E$_O$	−9.12
TS-nP$_\alpha$	6.52
PC-nP$_\alpha$	−18.63
TS-nP$_\beta$	6.18
PC-nP$_\beta$	−12.82
TS-nP$_\gamma$	7.53
PC-nP$_\gamma$	−11.46
TS-nP$_O$	9.83
PC-nP$_O$	−8.70
TS-iP$_\alpha$	5.64
PC-iP$_\alpha$	−19.58
TS-iP$_\beta$	8.82
PC-iP$_\beta$	−10.22
TS-iP$_O$	9.02
PC-iP$_O$	−8.92
TS-nB$_\alpha$	5.95
PC-nB$_\alpha$	−18.93
TS-nB$_\beta$	5.88
PC-nB$_\beta$	−12.98
TS-nB$_\gamma$	5.39
PC-nB$_\gamma$	−14.17
TS-nB$_O$	9.21
PC-nB$_O$	−8.99

In addition, rate coefficients were also calculated, using an estimation technique developed by Kwok and Atkinson,[48] which uses the presently available database to update the structure–activity relationship (SAR) method proposed by Atkinson[49] and latter extended by Atkinson[50] for the calculation of rate constants for the gas-phase reactions of the OH radical with organic compounds. The results are reported in Table 6.

$CH_3OH + OH$

The overall rate coefficient at 298 K calculated in this work (Table 4) agrees reasonably well with the values recommended by Atkinson *et al.*,[9] DeMore *et al.*[10] and Tsang,[51] $(9.3 \pm 2.3) \times 10^{-13}$, 8.95×10^{-13} and 1.69×10^{-13} cm^3 $molecule^{-1}$ s^{-1} respectively. It also shows good agreement with the value of 6.16×10^{-13} cm^3 $molecule^{-1}$ s^{-1}, estimated using the Kwok and Atkinson approach[48] (Table 6). It also agrees with some experimental determinations reported in the last two decades.[3,52–59] The rate coefficient for the formation of the hydroxymethyl radical (k_α) is larger than that of the competing channel (k_O) at any temperature in the range considered in this study. This result is in line with available experimental data. The alpha branching ratio ($\Gamma_\alpha = k_\alpha/k$) goes from 0.61 to 0.87, and it was found equal to 0.64 at 298 K (Table 5). Taking into account that these values of Γ_α are underestimated, and so are the overall rate coefficient (Table 1), it can be assumed that our k_α is underestimated.

A study of the rate coefficient temperature dependence was performed and the data derived in this work was expressed by a two parameter fit [$k = A\exp(-B/T)$] (Table 7). A good agreement between the theoretical and recommended[9] Arrhenius equations was found. The overall Arrhenius (E^{Arr}) activation energy was found to be 0.44 kcal/mol and the pre-exponential factor (A) equal to 1.32×10^{-12} cm^3 $molecule^{-1}$ s^{-1}. The E^{Arr} theoretical value is within the recommended reliability limits (Table 1) while the value of A is underestimated by a factor of 2.4, compared to the recommended one.[9] This dependence was also studied for the two independent channels. For the alpha channel the fit showed a small, but positive exponential parameter, while the corresponding to the hydroxylic channel is slightly negative. In addition there is a tunneling effect for both channels, with the hydroxylic transmition coefficient about twenty times larger than the alpha one (Table 5). Consequently, the finding that $k_\alpha > k_O$ is mainly caused by the appreciably larger value of A_α, compared to A_O. Since the pre-exponential factors can also be written as: $A = \frac{k_B T}{h}\exp\left(\frac{\Delta S^{\ddagger}}{R}\right)$, where ΔS represents the activation entropy, the difference between both pre-exponential factors can be explained by the features of the corresponding transition structures and by the larger tunneling of the hydroxylic channel. The **TS-M$_\alpha$** was found to be earlier, and thus looser than **TS-M$_O$** (Table 2) causing the entropy in the former one to be larger than the entropy in the latter one, and consequently $\Delta S_\alpha^{\ddagger} > \Delta S_O^{\ddagger}$. To simplify, we will refer to the entropy influence on the pre-exponential factor as entropic contribution. The disparity between the transmition coefficients of both channels causes a larger decreasing in the energy barrier of the second step of the reaction (E_2^*) for the hydroxylic channel compared to the alpha one, being $E_\alpha^{Arr} > E_O^{Arr}$ while the apparent energy barriers have the following order $E_\alpha^* < E_O^*$. The larger hydroxylic tunneling not only decreases the activation energy, but it also slightly reduces the pre-exponential factor. According to the above discussed results a curvature in the Arrhenius plot should be expected.

Table 4 CTST overall rate coefficients (cm^3 $molecule^{-1}$ s^{-1}) for C_1–C_4 alcohol + OH radical gas phase reactions

T	CH_3OH	C_2H_5OH	n-C_3H_7OH	i-C_3H_7OH	n-C_4H_9OH
290	7.15×10^{-13}	2.51×10^{-12}	4.36×10^{-12}	4.47×10^{-12}	7.67×10^{-12}
298.15	$\mathbf{6.82 \times 10^{-13}}$	$\mathbf{2.40 \times 10^{-12}}$	$\mathbf{4.04 \times 10^{-12}}$	$\mathbf{4.19 \times 10^{-12}}$	$\mathbf{6.88 \times 10^{-12}}$
310	6.51×10^{-13}	2.28×10^{-12}	3.70×10^{-12}	3.87×10^{-12}	6.01×10^{-12}
320	6.36×10^{-13}	2.21×10^{-12}	3.48×10^{-12}	3.66×10^{-12}	5.45×10^{-12}
340	6.27×10^{-13}	2.13×10^{-12}	3.17×10^{-12}	3.34×10^{-12}	4.67×10^{-12}
360	6.37×10^{-13}	2.10×10^{-12}	2.98×10^{-12}	3.12×10^{-12}	4.16×10^{-12}
380	6.61×10^{-13}	2.10×10^{-12}	2.87×10^{-12}	2.97×10^{-12}	3.83×10^{-12}
400	6.95×10^{-13}	2.12×10^{-12}	2.81×10^{-12}	2.87×10^{-12}	3.62×10^{-12}
420	7.38×10^{-13}	2.17×10^{-12}	2.79×10^{-12}	2.80×10^{-12}	3.47×10^{-12}
440	7.87×10^{-13}	2.22×10^{-12}	2.80×10^{-12}	2.76×10^{-12}	3.39×10^{-12}
460	8.43×10^{-13}	2.30×10^{-12}	2.83×10^{-12}	2.74×10^{-12}	3.34×10^{-12}
480	9.06×10^{-13}	2.38×10^{-12}	2.88×10^{-12}	2.74×10^{-12}	3.33×10^{-12}
500	9.74×10^{-13}	2.47×10^{-12}	2.95×10^{-12}	2.76×10^{-12}	3.34×10^{-12}

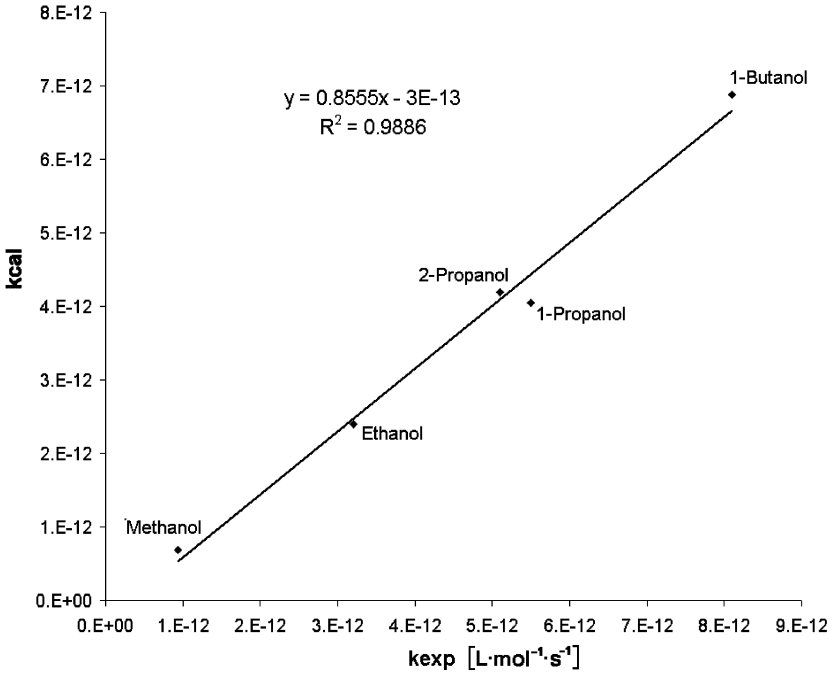

Fig. 7 Linear correlation for calculated *versus* experimental rate coefficients (cm^3 $molecule^{-1}$ s^{-1}).

Two features of the barrier of the hydroxylic hydrogen abstraction barrier are responsible for the large tunneling factor: (i) the larger imaginary frequency (ν) of this path (2316.6 cm^{-1} compared to 1349.2 cm^{-1}) leads to a narrower barrier; and (ii) E^*_{2O} is larger than $E^*_{2\alpha}$ by about 1 kcal mol^{-1}. The magnitude of ν has an inverse relation with the amplitude of the H-abstraction motion. This is related to the distance between the atom originally linked to the abstracted H and the atom which is performing the abstraction. The $C_\alpha \cdots O_{II}$ distance in **TS-M$_\alpha$** and the $O_I \cdots O_{II}$ distance in **TS-M$_O$**, with the former equal to 2.52 Å and the latter equal to 2.23 Å. From now on, we are going to refer to this kind of distance as a motion distance for simplifying purposes.

$C_2H_5OH + OH$

The rate coefficient corresponding to the alpha channel (k_α) was found larger than those of the other competing channels (k_β and k_O) at any temperature of this study, with the channel reactivity order: $k_\alpha > k_O > k_\beta$. The alpha branching ratio (Γ_α) goes from 0.76 to 0.90, over the studied temperature range, and it was found equal to 0.78 at 298 K (Table 5). Meier *et al.*[53] determined that at room temperature $\Gamma_\alpha = 0.75 \pm 0.15$; our result has an excellent agreement with the value reported by them, but it is slightly underestimated compared to the recommended value of 0.90 (Table 1). The overall rate coefficient at 298 K calculated in this work (Table 4) is in

Table 5 Overall CTST Arrhenius parameters for C_1–C_4 alcohol + OH radical gas phase reactions, Arrhenius activation energies and pre-exponential factors of each channel determined over the temperature range 290–500 K. Each channel rate coefficient, tunneling factor and branching fractions are reported at 298.15 K

	CH_3OH	C_2H_5OH	n-C_3H_7OH	i-C_3H_7OH	n-C_4H_9OH
E^{Arr}/kcal mol^{-1}	0.44	−0.02	−0.54	−0.68	−1.14
A/cm^3 $molecule^{-1}$ s^{-1}	1.32×10^{-12}	2.20×10^{-12}	1.53×10^{-12}	1.30×10^{-12}	9.27×10^{-13}
k_α	4.37×10^{-13}	1.88×10^{-12}	2.05×10^{-12}	3.39×10^{-12}	1.84×10^{-12}
k_β	—	1.69×10^{-13}	1.59×10^{-12}	4.33×10^{-13}	1.50×10^{-12}
k_γ	—	—	2.14×10^{-13}	—	3.31×10^{-12}
k_O	2.45×10^{-13}	3.53×10^{-13}	1.84×10^{-13}	3.74×10^{-13}	2.31×10^{-13}
E^{Arr}_α	0.91	0.20	0.02	−0.57	0.06
E^{Arr}_β	—	−0.79	−1.68	−0.87	−1.85
E^{Arr}_γ	—	—	−0.64	—	−2.19
E^{Arr}_O	−1.15	−1.51	−0.96	−1.79	−1.08
A_α	1.93×10^{-12}	2.53×10^{-12}	2.04×10^{-12}	1.26×10^{-12}	1.98×10^{-12}
A_β	—	4.02×10^{-14}	8.79×10^{-14}	8.98×10^{-14}	6.24×10^{-14}
A_γ	—	—	6.85×10^{-14}	—	7.82×10^{-14}
A_O	3.19×10^{-14}	2.45×10^{-14}	3.23×10^{-14}	1.98×10^{-14}	3.36×10^{-14}
$\kappa_2(\alpha)$	4.28	1.96	2.09	1.15	1.55
$\kappa_2(\beta)$	—	32.17	8.20	29.91	8.44
$\kappa_2(\gamma)$	—	—	6.67	—	7.21
$\kappa_2(O)$	87.53	120.48	138.20	95.71	113.58
Γ_α	0.64	0.78	0.51	0.81	0.27
Γ_β	—	0.07	0.39	0.10	0.22
Γ_γ	—	—	0.05	—	0.48
Γ_O	0.36	0.15	0.05	0.09	0.03

Table 6 Rate coefficients and branching ratios calculated using the estimation technique developed by Kwok and Atkinson[46]

	Methanol	Ethanol	1-Propanol	2-Propanol	1-Butanol
k/cm^3 molecule^{-1} s^{-1}	6.16×10^{-13}	3.61×10^{-12}	5.51×10^{-12}	7.30×10^{-12}	6.92×10^{-12}
k_α	4.76×10^{-13}	3.27×10^{-12}	4.02×10^{-12}	6.79×10^{-12}	4.02×10^{-12}
k_β	—	1.67×10^{-13}	1.15×10^{-12}	3.35×10^{-13}	1.41×10^{-12}
k_γ	—	—	1.63×10^{-13}	—	1.15×10^{-12}
k_O	1.40×10^{-13}	1.72×10^{-13}	1.72×10^{-13}	1.72×10^{-13}	1.72×10^{-13}
Γ_α	0.77	0.91	0.73	0.93	0.58
Γ_β	—	0.05	0.21	0.05	0.20
Γ_γ	—	—	0.03	—	0.17
Γ_O	0.23	0.05	0.03	0.02	0.02

excellent agreement with the values recommended by Atkinson *et al.*[9] and DeMore *et al.*,[10] $(3.2 \pm 0.8) \times 10^{-12}$ and 3.18×10^{-12} cm^3 molecule^{-1} s^{-1} respectively, in addition to other experimental determinations.[3,53,56–61] It also agrees well with the value of 3.61×10^{-12} cm^3 molecule^{-1} s^{-1}, estimated using the Kwok and Atkinson approach[48] (Table 6).

The temperature dependence over the 290–500 K range of the overall rate coefficient, as well as the corresponding to the three competing channels were studied, the Arrhenius plots of calculated k values were linearly fitted and a good agreement with the recommended two parameters expression[9] was obtained. The overall E^{Arr} was found to be almost zero and within the recommended reliability limits (Table 1). The overall theoretical pre-exponential factor is underestimated by a factor of 1.9, compared to the recommended value.[9] The alpha channel showed a small negative exponential factor (B_α), while B_β and B_O were found positive and the latter larger than the former one (Table 7), *i.e.* the order in Arrhenius activation energy is $E_O^{Arr} < E_\beta^{Arr} < E_\alpha^{Arr}$, which is just the opposite than that of the apparent energy barrier: $E_\alpha^* < E_\beta^* < E_O^*$ (Table 2); this inversion is caused by the tunneling effect. The hydroxylic transmission coefficient (κ_O) is sixty times larger than κ_α and about four times larger than κ_β. The imaginary frequencies of these channels are ν(**TS-E$_\alpha$**) = 1029.7, ν(**TS-E$_\beta$**) = 1944.0, and ν(**TS-E$_O$**) = 2341.5 cm^{-1}, while the motion distances are $d(C_\alpha \cdots O_{II}) = 2.54$ Å, $d(C_\beta \cdots O_{II}) = 2.45$ Å, and $d(C_O \cdots O_{II}) = 2.23$ Å. As well as in the $CH_3OH + OH$ reaction, a curvature in the Arrhenius plot is expected. The fact that the alpha channel has the largest k is mainly related to entropic contributions; this is confirmed by its pre-exponential factor, which is two orders of magnitude larger than those of the beta and hydroxylic channels (Table 5).

Table 7 Two-parameter kinetics description of the C_1–C_4 alcohol + OH reactions (cm^3 molecule^{-1} s^{-1}). Error limits represent 2 standard deviations (from the least-squares analysis)

	$k = A\exp(-B/T)$
CH_3OH	
k	$(1.32 \pm 0.22) \times 10^{-12}\exp[(-220 \pm 60)/T]$
k_α	$(1.93 \pm 0.20) \times 10^{-12}\exp[(-460 \pm 38)/T]$
k_O	$(3.19 \pm 0.68) \times 10^{-14}\exp[(577 \pm 71)/T]$
C_2H_5OH	
k	$(2.20 \pm 0.24) \times 10^{-12}\exp[(10 \pm 38)/T]$
k_α	$(2.53 \pm 0.19) \times 10^{-12}\exp[(-100 \pm 26)/T]$
k_β	$(4.02 \pm 0.86) \times 10^{-14}\exp[(398 \pm 70)/T]$
k_O	$(2.45 \pm 0.60) \times 10^{-14}\exp[(761 \pm 78)/T]$
n-C_3H_7OH	
k	$(1.53 \pm 0.19) \times 10^{-12}\exp[(270 \pm 43)/T]$
k_α	$(2.04 \pm 0.16) \times 10^{-12}\exp[(-11 \pm 28)/T]$
k_β	$(8.79 \pm 0.12) \times 10^{-14}\exp[(844 \pm 44)/T]$
k_γ	$(6.85 \pm 0.84) \times 10^{-14}\exp[(321 \pm 42)/T]$
k_O	$(3.23 \pm 0.81) \times 10^{-14}\exp[(482 \pm 82)/T]$
i-C_3H_7OH	
k	$(1.30 \pm 0.11) \times 10^{-12}\exp[(337 \pm 30)/T]$
k_α	$(1.26 \pm 0.08) \times 10^{-14}\exp[(286 \pm 21)/T]$
k_β	$(8.98 \pm 1.84) \times 10^{-14}\exp[(439 \pm 68)/T]$
k_O	$(1.98 \pm 0.44) \times 10^{-14}\exp[(843 \pm 73)/T]$
n-C_4H_9OH	
k	$(9.27 \pm 1.34) \times 10^{-13}\exp[(576 \pm 50)/T]$
k_α	$(1.98 \pm 0.13) \times 10^{-12}\exp[(-31 \pm 23)/T]$
k_β	$(6.24 \pm 0.76) \times 10^{-14}\exp[(929 \pm 42)/T]$
k_γ	$(7.82 \pm 0.88) \times 10^{-14}\exp[(1100 \pm 40)/T]$
k_O	$(3.36 \pm 0.77) \times 10^{-14}\exp[(542 \pm 76)/T]$

n-C_3H_7OH + OH

Similarly to the methanol and ethanol reactions, in this case the rate coefficient corresponding to the alpha channel (k_α) is larger than those of the other competing channels (k_β, k_γ and k_O) at any temperature of this study, with the different channels reactivity order: $k_\alpha > k_\beta > k_\gamma > k_O$. The overall rate coefficient at 298 K calculated in this work (Table 4) is in good agreement with the $(5.5 \pm 1.7) \times 10^{-12}$ cm^3 molecule^{-1} s^{-1} value recommended by Atkinson *et al.*,[9] as well as with the experimental data available.[3,59,62–64] It also shows a good agreement with the value of 5.51×10^{-12} cm^3 molecule^{-1} s^{-1}, estimated using the Kwok and Atkinson approach[48] (Table 6). The alpha branching ratio (Γ_α) goes from 0.48 to 0.73, over the studied temperature range, and it was found equal to 0.51 at 298 K (Table 5). This value is underestimated compared to that of 0.73 derived from the data in ref. 7.

The Arrhenius plots obtained from the calculation of the overall rate coefficients, as well as those corresponding to the four competing channels, over the 290–500 K temperature range, were linearly fitted. The overall E^{Arr} was found to be slightly negative (−0.54 kcal mol^{-1}). Using this value and the correlation between E_{Calc}^{Arr} and E_{Exp}^{Arr}, a corrected activation energy value of −0.28 kcal mol^{-1} is proposed. It should be expected the latter value to be closer than the former one to experimental determinations. The alpha channel showed an almost zero exponential factor (B_α), while B_β, B_γ, and B_O were found positive (Table 7). The order in Arrhenius activation energy is $E_\beta^{Arr} < E_O^{Arr} < B_\gamma^{Arr} < E_\alpha^{Arr}$, which is different to that of the apparent energy barrier: $E_\alpha^* < E_\beta^* < E_\gamma^* < E_O^*$ (Table 2). This effect is caused by tunneling. For this reaction the hydroxylic transmission coefficient (κ_O) is 66 times larger than κ_α, 17 times larger than κ_β, and 21 times larger than κ_γ. The imaginary frequencies of these channels are: ν(**TS-nP$_\alpha$**) = 1071.5, ν(**TS-nP$_\beta$**) = 1417.4, ν(**TS-nP$_\gamma$**) = 1512.0, and ν(**TS-nP$_O$**) = 2343.8 cm^{-1} and the motion distances are: $d(C_\alpha \cdots O_{II}) = 2.53$ 2.53 Å, $d(C_\beta \cdots O_{II}) = 2.50$ Å, $d(C_\gamma \cdots O_{II}) = 2.51$ Å, and $d(C_O \cdots O_{II}) = 2.23$ Å. As well as in the previous discussed reactions, a curved Arrhenius plot is expected. The fact that the alpha channel has the largest k is predominantly related with entropic contributions, which is corroborated by its pre-exponential factor, which is two orders larger than those of the beta, gamma and hydroxylic channels (Table 5).

A similar correlation that the one between E_{Calc}^{Arr} and E_{Exp}^{Arr} was also performed for the pre-exponential factor, in order

to propose a corrected Arrhenius expression and to predict an expected temperature dependence for the n-$C_3H_7OH + OH$ reaction. The two-parameter expressions obtained without and with this correction are $k_{1\text{-Prop}} = (1.53 \pm 0.19) \times 10^{-12}\exp[(270 \pm 43)/T]$ and $k_{1\text{-Prop}} = 3.06 \times 10^{-12}\exp(140/T)$ cm^3 $molecule^{-1}$ s^{-1}, respectively. These equations agree reasonably well with the only temperature dependence study on the n-$C_3H_7OH\cdot + OH$ reaction reported in the literature $(4.68 \pm 0.64) \times 10^{-12}\exp[(68 \pm 41)/T]$,[64] and logically the agreement is better with the corrected expression. The small discrepancies between the two parameters expression reported in ref. 64 and ours is artificially increased by the fact that the temperature range studied in both works are different.

i-C_3H_7OH + OH

The rate coefficient corresponding to the α channel (k_α) is larger than those of the other competing channels (k_β and k_O) at any temperature of this study, with the channel reactivity order: $k_\alpha > k_\beta > k_O$. The overall rate coefficient at 298 K calculated in this work (Table 4) is in good agreement with the $(5.1 \pm 1.1) \times 10^{-12}$ cm^3 $molecule^{-1}$ s^{-1} value recommended by Atkinson *et al.*,[9] as well as with the experimental of the last few decades.[3,59,64–66] It also agrees well with the value of 7.30×10^{-12} cm^3 $molecule^{-1}$ s^{-1}, estimated using the Kwok and Atkinson approach[48] (Table 6). The only available measure of the branching ratios is $\Gamma_\beta = 0.12$ by Dunlop and Tully.[65] Our calculations developed a value of $\Gamma_\beta = 0.10$ (Table 5), this excellent agreement supports the reliability of the calculated alpha and hydroxylic branching ratios, which has not been previously reported.

The dependence of the overall rate coefficient with temperature, as well as the corresponding to the three competing channels were studied, over the 290–500 K range, and the k values obtained plotted into Arrhenius plots. A reasonable agreement with the recommended two parameters expression[9] was obtained and the overall E^{Arr} was found to be negative and within the recommended reliability limits (Tables 1 and 5). The overall theoretical pre-exponential factor is underestimated by a factor of 2.1, compared to the recommended value.[9] All the channels showed positive exponential factors (Table 7), and the order in Arrhenius activation energy is $E_O^{Arr} < E_\beta^{Arr} < E_\alpha^{Arr}$, which is just the opposite than that of the apparent energy barrier: $E_\alpha^* < E_\beta^* < E_O^*$ (Table 2); this inversion is caused by the tunneling effect. The hydroxylic transmition coefficient (κ_O) is about eighty times larger than κ_α and about three times larger than κ_β. Consequently, the fact that the alpha channel has the largest k is mainly related with entropic contributions, which can be corroborated by its pre-exponential factor, which is about one order larger than the beta one and more than one order and a half than that of the hydroxylic channel (Table 5). The imaginary frequencies of the different competitive channels are: ν(**TS-iP$_\alpha$**) = 732.4, ν(**TS-iP$_\beta$**) = 1950.1, and ν(**TS-iP$_O$**) = 2346.6 cm^{-1}, while the motion distances are: $d(C_{\alpha\cdot}\cdots O_{II}) = 2.56$ Å, $d(C_\beta\cdots O_{II}) = 2.45$ Å, and $d(C_O\cdots O_{II}) = 2.24$ Å. As well as in the previous discussed reactions, a curvature in the Arrhenius plot is expected.

n-C_4H_9OH + OH

This is a very peculiar case among the alcohol + OH reactions. The rate coefficient corresponding to the gamma channel (k_γ) was found larger than those of the other competing channels (k_α, k_β and k_O) over a temperature range from 290 to 350 K, while the alpha channel was found predominant over the range 350–500 K. The larger k_α can be explained by the features of the transition structures (Fig. 5). The alpha (**TS-nB$_\alpha$**), beta (**TS-nB$_\beta$**) and gamma (**TS-nB$_\gamma$**) transition states show hydrogen bond like stabilizations, with the corresponding interaction distances: $d(O_I\cdots H_{O_{II}}) = 2.98$ Å, $d(O_{II}\cdots H_{O_I}) = 2.17$ Å, and $d(O_{II}\cdots H_{O_I}) = 1.93$ Å, respectively. The shortest distance in **TS-nB$_\gamma$** causes a larger stabilization, *i.e*: it shows a lower energy barrier and a larger rate coefficient.

The overall rate coefficient at 298 K calculated in this work (Table 4) is in good agreement with the $(8.1 \pm 2.4) \times 10^{-12}$ cm^3 $molecule^{-1}$ s^{-1} value recommended by Atkinson *et al.*,[9] as well as with the experimental data available.[3,59,63,64,67] It also agrees well with the value of 6.92×10^{-12} cm^3 $molecule^{-1}$ s^{-1}, estimated using the Kwok and Atkinson approach[48] (Table 6). As far as we know, there are not any previously reported results of the branching ratios. According to our results Γ_α goes from 0.25 to 0.59, Γ_β from 0.22 to 0.13, Γ_γ from 0.50 to 0.24, and Γ_O goes from 0.03 to 0.04, over the studied temperature range. The values of the calculated branching ratios at 298 K are reported in Table 5. The branching ratios obtained by the SAR approach[48] are shown in Table 6. However, new SAR substitution factors for hydroxyl compounds have been proposed by Bethel *et al*,[68] the authors considered the effects of the OH substituents on H atom abstraction at the α and β positions, with new factors of F(–OH) = 2.9 and F(–CH_2OH) = F(>CHOH) = F(≥COH) = 2.6. This updated approach gives more relevance to the beta abstractions and leads to new branching ratios of $\Gamma_\alpha = 0.43$, $\Gamma_\beta = 0.38$, $\Gamma_\gamma = 0.15$ and $\Gamma_O = 0.02$.

In addition, Wallington and Kurylo[69] have proven that in ketones there is a significant enhancement of the group reactivity toward OH for both CH_3 and CH_2 when moved from the α to β positions, with respect to the carbonyl group and this has been taking into account in the SAR method[48] by factors of F[–CH_2C(O)] = F[>CHC(O)] = F[≥CC(O)] = 3.9. Beta carbons in ketones and gamma carbons in alcohols are both two carbon atoms apart from the oxygen atom, in fact the distance $H_{\beta\cdot}\cdots O$ in ketones and $H_{\gamma\cdot}\cdots O$ in alcohols were found to be equal to 2.69 and 2.63 Å, respectively, according to BHandHLYP/6-311G(d,p) fully optimized geometries. Therefore, it seems reasonable to assume that new corrections to SAR should be made. As a rough approximation we have considered F(–CH_2–) = F(>CH–) = F(>C<) = 1.23,[48] F(–OH) = 2.9[68] and F(–CH_2CH_2OH) = F(>$CHCH_2OH$) = F(≥CCH_2-OH) = 3.9, which is the equivalent factor to that for beta sites in ketones. Using these factors the rate coefficients are $k_{tot} = 8.73 \times 10^{-12}$, $k_\alpha = 3.33 \times 10^{-12}$, $k_\beta = 1.41 \times 10^{-12}$, $k_\gamma = 3.64 \times 10^{-12}$, $k_\delta = 1.67 \times 10^{-13}$ and $k_O = 1.72 \times 10^{-13}$ cm^3 $molecule^{-1}$ s^{-1}; leading to branching ratios of $\Gamma_\alpha = 0.38$, $\Gamma_\beta = 0.16$, $\Gamma_\gamma = 0.42$, $\Gamma_\delta = 0.02$ and $\Gamma_O = 0.02$. The rate coefficients obtained this way are in as good agreement as those obtained using the previously proposed factors with the recommended values but they additionally include the enhanced reactivity of the gamma site found in this work.

Recently an experimental study was carried out on the OH initiated oxidation of 1-butanol by Cavalli *et al.*[67] and the product formation yields were reported (butanal = 0.518 ± 0.071, propanal = 0.234 ± 0.035, acetaldehyde = 0.127 ± 0.022, formaldehyde = 0.434 ± 0.024, 4-hydroxy-2-butanone = 0.05 ± 0.01). The corresponding normalized values would be butanal = 0.380, propanal = 0.172, acetaldehyde = 0.093, formaldehyde = 0.318, and 4-hydroxy-2-butanone = 0.037. According to scheme 1 on reference 67 the entire butanal, propanal and acetaldehyde formation are due to alpha, beta and gamma abstractions, respectively. The 4-hydroxy-2-butanone is also caused by the gamma abstraction. However, the formaldehyde is produced by further reaction after beta or gamma abstractions occur, it can also be produced by delta abstractions, which is a very minor path. Consequently, according to Cavalli *et al.*'s results it can be said that $\Gamma_\alpha = 0.38$, while the values of $\Gamma_\beta = 0.17$ and $\Gamma_\gamma = 0.13$ are only lower limits. Further experiments could clarify in what proportion the beta and gamma channels contribute to the formaldehyde yielding.

According to the discussion above, at this point and taking into account all the results on the 1-butanol + OH reaction, it can only be certainly established that the gamma site reactivity is higher than the previously thought. In addition it is possible that this path successfully competes with the alpha one.

The Arrhenius plots were obtained from the calculation of the overall rate coefficients, as well as the corresponding to the four competing channels, over the 290 – 500 K temperature range. The overall E^{Arr} was found to be negative (−1.14 kcal mol^{-1}). Using the calculated value and the correlation between E^{Arr}_{Calc} and E^{Arr}_{Exp} a corrected activation energy value of −0.88 kcal/mol is obtained. It is anticipated that this value should be closer to future experimental determinations than the uncorrected one. The overall pre-exponential factor (A) was found to be 9.27×10^{-13} cm^3 molecule^{-1} s^{-1}. There is not any experimental A to compare, but similar results in the C_1–C_3 alcohols suggest that this value is underestimated by a factor of about 2.

The alpha channel showed a negative, and almost zero, exponential factor (B_α), while B_β, B_γ, and B_O were found positive (Table 7). The order in Arrhenius activation energy is $E^{Arr}_\gamma < E^{Arr}_\beta < B^{Arr}_O < E^{Arr}_\alpha$, which is different to that of the apparent: $E^*_\gamma < E^*_\beta < E^*_\alpha < E^*_O$ (Table 2). This change is caused by the small tunneling effect in the alpha channel. The hydroxylic transmition coefficient (κ_O) is 74 times larger than κ_α. The imaginary frequencies are: ν(**TS-nBα**) = 996.2, ν(**TS-nBβ**) = 1762.9, ν(**TS-nBγ**) = 1760.3, and ν(**TS-nBO**) = 2364.3 cm^{-1} and the motion distances are: $d(C_\alpha \cdots O_{II})$ = 2.54 2.54 Å, $d(C_\beta \cdots O_{II})$ = 2.45 Å, $d(C_\gamma \cdots O_{II})$ = 2.54 Å, and $d(C_O \cdots O_{II})$ = 2.23 Å. As well as in the previous discussed reactions, a curved Arrhenius plot is expected.

The fact that the gamma channel has the largest k at low temperatures is related to energetic contributions, *i.e.*: this channel has the lowest energy barrier. As the temperature increases the relevance of the energetic contribution decreases and the alpha channel becomes dominant due to the entropic contribution, its pre-exponential factor is the largest one, about two orders larger than that of any other channel (Table 5). The gamma predominance at room temperatures, also suggest an additional explanation to the findings of Oh and Andino,[11] that the presence of ammonium sulfate aerosols promote the reactions of OH radicals only with aliphatic alcohols containing fewer than four carbon atoms. The fact that the preferred site for the hydrogen abstraction, at this temperature, is the gamma one, implies that the interaction of the aerosol with the functional group of the alcohols is apart enough to provoke any appreciable effect on the rate coefficient.

Finally, a similar correlation that the one between E^{Arr}_{Calc} and E^{Arr}_{Exp} was also performed for the pre-exponential factor (A^{Arr}_{Calc} *vs.* A^{Arr}_{Exp}), in order to propose a corrected Arrhenius expression and to predict temperature dependence of the n-C_4H_9OH + OH reaction that should be expected experimentally. The best fit equation was, $A^{Arr}_{Calc} = 0.666A^{Arr}_{Exp} + 6 \times 10^{-13}$, $\times 10^{-13}$, with a correlation coefficient (R^2) equal to 0.91. Using both correlations, a two parameters equation is proposed: $k_{1\text{-But}} = 2.14 \times 10^{-12}\exp(440/T)$ cm^3 molecule^{-1} s^{-1}, compared to the uncorrected expression $k_{1\text{-But}} = (9.27 \pm 1.34) \times 10^{-13}\exp[(576 \pm 50)/T]$. Both equations are in a reasonable agreement with the only temperature dependence study on the n-$C_3H_7OH^{\bullet}$ + OH reaction reported in literature $(5.30 \pm 1.62) \times 10^{-12}\exp[(146 \pm 92)]$,[64] taking into account the different studied temperature range, and logically the agreement is better with the corrected expression.

Conclusions

Very stable pre-reactive complexes (RC) for all the abstraction paths were found, showing unambiguously that the mechanism of each reaction channel is complex with a first step leading to the RC formation and a second step yielding the corresponding radical and water. The RC formation, together with the appreciable transmition coefficient explains the negative apparent Arrhenius activation energies.

The hydroxylic channels of the studied alcohols show the largest transmition coefficients of the all competitive channels causing a large decrease in the hydroxylic Arrhenius activation energy (E^{Arr}). This effect causes the apparent energy barriers to be different than the E^{Arr}.

At any temperature of this study, the rate coefficient for the formation of the alpha radical (k_α) is significantly larger than that of the competing channels, for C_1–C_3 alcohols. For 1-butanol, the rate coefficient corresponding to the gamma channel was found as the largest one, over a temperature range from 290 to 350 k, while the alpha channel was found predominant over the range 350–500 K.

The results of our theoretical studies of the alcohol + OH reactions are consistent with the data gathered through various experimental studies of the OH-initiated photo oxidation of alcohols. Previous experimental works indicate product distributions that are consistent with attack at the alpha position for C_1–C_3 alcohols.[52–56,58,65] In addition, our theoretical studies help to explain the heterogeneous studies of Oh and Andino[11] for >C_3 alcohols. The finding that the preferred site for the n-C_4H_9OH hydrogen abstraction is the gamma one, at room temperature, supports the observation by Oh and Andino that the presence of ammonium sulfate aerosols does not promote the reactions of OH radicals with aliphatic alcohols containing four or more carbon atoms.

Acknowledgements

The authors gratefully acknowledge the financial support from the Instituto Mexicano del Petróleo (IMP) through programs G00058, D888 and D12. We also thank the IMP Computing Center for supercomputer time on SGI Origin 2000. We thank Professors W. T. Duncan, R. L. Bell and T. N. Truong for providing the Rate program through Internet. The authors also thank to Profesor Jean M. Andino for the valuable discussion about the studied reaction.

References

1 T. E. Graedel, D. T. Hawkings, L. D. Claxton, *Atmospheric Chemical Compounds*, Academic Press, Orlando, 1986.
2 J. H. Seinfield, J. M. Andino, F. M. Bowman, H. J. Frostner and S. Pandis, *Adv. Chem. Eng.*, 1994, **19**, 325–405.
3 T. J. Wallington and M. J. Kurylo, *Int. J. Chem. Kinet.*, 1987, **19**, 1015–1023.
4 B. Picquet, S. Heroux, A. Chebbi, J. Doussin, R. Durand-Jolibois, A. Monod, H. Loirat and P. Carlier, *Int. J. Chem. Kinet.*, 1998, **30**, 839–847.
5 Guidance on Estimating Motor Vehicle Emission Reduction from the Use of Alternative Fuels and Fuel Blends; U.S.E.P.A.; Report No. 1 APA-AA-TSS-PA-87-4; Ann Arbor, Michigan, 1998.
6 E. Grosjean, D. Grosjean, R. Gunawardena and R. A. Rasmussen, *Environ. Sci. Technol.*, 1998, **32**, 736–742.
7 R. Atkinson, *J. Phys. Chem. Ref. Data*, Monograph 2, 1994, 1–134.
8 R. Atkinson, D. L. Baulch, R. A. Cox, R. F. Jr. Hampson, J. A. Kerr, M. J. Rossi and J. Troe, *J. Phys. Chem. Ref. Data*, 1997, **26**, 521.
9 R. Atkinson, D. L. Baulch, R. A. Cox, R. F. Jr. Hampson, J. A. Kerr, M. J. Rossi and J. Troe, *J. Phys. Chem. Ref. Data*, 1999, **28**(2), 191.
10 W. B. DeMore, S. P. Sander, D. M. Golden, R. F. Hampson, M. J. Kurylo, C. J. Howard, A. R. Ravishankara, C. E. Kolb and M. J. Molina, *JPL Publication*, 1997, **97**, 4.
11 S. Oh and J. M. Andino, *Int. J. Chem. Kinet.*, 2001, **33**(7), 422–430.
12 P. J. Robinson and K. A. Holbrook, *Unimolecular Reactions*, Wiley-Interscience, London, 1972.

13 M. J. Frisch, G. W. Trucks, H. B. Schlegel, G. E. Scuseria, M. A. Robb, J. R. Cheeseman, V. G. Zakrzewski, J. A. Montgomery Jr., R. E. Stratmann, J. C. Burant, S. Dapprich, J. M. Millam, A. D. Daniels, K. N. Kudin, M. C. Strain, O. Farkas, J. Tomasi, V. Barone, M. Cossi, R. Cammi, B. Mennucci, C. Pomelli, C. Adamo, S. Clifford, J. Ochterski, G. A. Petersson, P. Y. Ayala, Q. Cui, K. Morokuma, D. K. Malick, A. D. Rabuck, K. Raghavachari, J. B. Foresman, J. Cioslowski, J. V. Ortiz, B. B. Stefanov, G. Liu, A. Liashenko, P. Piskorz, I. Komaromi, R. Gomperts, R. L. Martin, D. J. Fox, T. Keith, M. A. Al-Laham, C. Y. Peng, A. Nanayakkara, C. Gonzalez, M. Challacombe, P. M. W. Gill, B. Johnson, W. Chen, M. W. Wong, J. L. Andres, M. Head-Gordon, E. S. Replogle and J. A. Pople, Gaussian 98 Revision A.3, Gaussian, Inc., Pittsburgh, PA., 1998.
14 Æ. Frisch and M. J. Frisch, *Gaussian 98 Users Reference*, Gaussian Inc., Pittsburgh, PA, 1998, p. 75.
15 Q. Zhang, R. Bell and T. N. Truong, *J. Phys. Chem.*, 1995, **99**, 592.
16 J. L. Durant, *Chem. Phys. Lett.*, 1996, **256**, 595.
17 B. Braýda and P. C. Hiberty, *J. Phys. Chem. A.*, 1998, **102**, 7872.
18 G. N. Sastry, T. Bally, V. Hrouda and P. Carsky, *J. Am. Chem. Soc.*, 1998, **120**, 9323.
19 J. Oxgaard and O. Wiest, *J. Phys. Chem. A*, 2001, **105**, 8236.
20 B. M. Rice, S. V. Pai and C. F. Chabalowski, *J. Phys. Chem. A*, 1998, **102**, 6950.
21 Y. Zhang, C. Y. Zhao and X. Z. You, *J. Phys. Chem. A*, 1997, **101**, 2879.
22 K. Furuya, Y. Inagaki, H. Torii, Y. Furukawa and M. Tasumi, *J. Phys. Chem. A*, 1998, **102**, 8413.
23 W.-J. Ding and D.-C. Fang, *J. Org. Chem.*, 2001, **66**(20), 6673.
24 J. R. Alvarez-Idaboy, A. Galano, G. Bravo-Pérez and M. E. Ruiz, *J. A. Chem. Soc.*, 2001, **123**(34), 8387.
25 H. Eyring, *J. Chem. Phys.*, 1935, **3**, 107.
26 D. G. Truhlar, W. L. Hase and J. T. Hynes, *J. Phys. Chem.*, 1983, **87**, 2264.
27 W. T. Duncan, R. L. Bell and T. N. Truong, *J. Comput. Chem.*, 1998, **19**, 1039.
28 C. Eckart, *Phys. Rev.*, 1930, **35**, 1303.
29 T. N. Truong and D. G. Truhlar, *J. Chem. Phys.*, 1990, **93**, 1761.
30 T. N. Truong, *J. Phys. Chem. B*, 1997, **101**, 2750.
31 T. N. Truong, W. T. Duncan and M. Tirtowidjojo, *Phys. Chem. Chem. Phys.*, 1999, **1**, 1061.
32 D. G. Truhlar, A. D. Isaacson, R. T. Skodje and B. C. Garrett, *J. Phys. Chem.*, 1982, **86**, 2252.
33 J. T. Jodkowski, M. T. Rayez and J. C. Rayez, *J. Phys. Chem. A.*, 1999, **103**, 3750.
34 N. Luo, D. C. Kombo and R. Osman, *J. Phys. Chem. A*, 1997, **101**, 926.
35 M. T. Rayez, J. C. Rayez and J. P. Sawerysyn, *J. Phys. Chem.*, 1994, **98**, 11 342.
36 A. Talhaoui, F. Louis, P. Devolder, B. Meriaux, J. P. Sawerysyn, M. T. Rayez and J. C. Rayez, *J. Phys. Chem.*, 1996, **100**(32), 13 531.
37 R. A. Loomis and M. I. Lester, *J. Chem. Phys.*, 1995, **103**, 4371.
38 M. I. Lester, B. V. Pond, D. T. Anderson, L. B. Harding and A. F. Wagner, *J. Chem. Phys.*, 2000, **113**(22), 9889.
39 I. W. M. Smith and A. R. Ravishankara, *J. Phys. Chem. A*, 2002, **106**, 4798.
40 J. R. Alvarez-Idaboy, N. Mora-Diez and A. Vivier-Bunge, *J. Am. Chem. Soc.*, 2000, **122**, 3715.
41 V. H. Uc, I. García-Cruz, A. Hernández-Laguna and A. Vivier-Bunge, *J. Phys. Chem. A.*, 2000, **104**, 7847.
42 J. R. Alvarez-Idaboy, N. Mora-Diez, R. J. Boyd and A. Vivier-Bunge, *J. Am. Chem. Soc.*, 2001, **123**, 2018.
43 A. Galano, J. R. Alvarez-Idaboy, L. A. Montero-Cabrera and A. Vivier-Bunge, *J. Comput. Chem.*, 2001, **22**(11), 1138.
44 A. Galano, J. R. Alvarez-Idaboy, G. Bravo-Pérez and M. E. Ruiz-Santoyo, *THEOCHEM*, in press.
45 D. L. Singleton and R. J. Cvetanovic, *J. Am. Chem. Soc.*, 1976, **98**, 6812.
46 M. J. Pilling, P. W. Seakins, *Reaction Kinetics*, Oxford University Press, New York, 1996.
47 K. J. Laidler, *Chemical Kinetics*, ed. Harper Collins Publishers, 1987, p. 98.
48 E. S. C. Kwok and R. Atkinson, *Atmos. Env.*, 1995, **29**(14), 1685.
49 R. Atkinson, *Chem. Rev.*, 1986, **86**, 69.
50 R. Atkinson, *Int. J. Chem Kinet.*, 1987, **19**, 799.
51 W. Tsang, *J. Phys. Chem. Ref. Data 16*, 1987, 471.
52 J. Hagele, K. Lorenz, D. Rhasa and R. Zellner, *Ber. Bunsen-Ges. Phys. Chem.*, 1983, **87**, 1023.
53 U. Meier, H. H. Grotheer, G. Riekert and Th. Just, *Ber. Bunsen-Ges. Phys. Chem.*, 1985, **89**, 325.
54 U. Meier, H. H. Grotheer and Th. Just, *Chem. Phys. Lett.*, 1984, **106**, 97.
55 W. P. Hess and F. P. Tully, *J. Phys. Chem.*, 1989, **93**, 1944.
56 J. A. McCaulley, N. Nelly, M. F. Golde and F. Kaufman, *J. Phys. Chem.*, 1989, **93**, 1014.
57 R. Atkinson, *Chem. Rev.*, 1986, **86**, 69.
58 J. F. Bott and N. Cohen, *Int. J. Chem. Kinet.*, 1991, **23**, 1075.
59 L. Nelson, O. Rattigan, R. Neavyn, H. Sidebottom, J. Treacy and O. J. Nielsen, *Int. J. Chem. Kinet.*, 1990, **22**, 1111.
60 W. P. Hess and F. P. Tully, *Chem. Phys. Lett.*, 1988, **152**, 183.
61 U. Meier, H. H. Grotheer, G. Riekert and Th. Just, *Chem. Phys. Lett.*, 1987, **133**, 162.
62 R. Overend and G. Paraskevopoulos, *J. Phys. Chem.*, 1978, **82**, 1329.
63 I. M. Campbell, D. F. McLaughlin and B. J. Handy, *Chem. Phys. Lett.*, 1976, **38**, 362.
64 M. Yujing and A. Mellouki, *Chem. Phys. Lett.*, 2001, **333**, 63.
65 J. R. Dunlop and F. P. Tully, *J. Phys. Chem.*, 1993, **97**, 6457.
66 V. W. Klopffer, R. Frank, E. G. Kohl and F. Haag, *Chem.-Ztg.*, 1986, **110**, 57.
67 F. Cavalli, H. Geiger, I. Barnes and K. H. Becker, *Environ. Sci. Technol.*, 2002, **36**, 1263.
68 H. L. Bethel, R. Atkinson and J. Arey, *Int. J. Chem. Kinet.*, 2001, **33**, 310.
69 T. J. Wallington and M. J. Kurylo, *J. Phys. Chem.*, 1987, **91**, 5050.